AN INTEGRATED EARTHQUAKE DAMAGE DETECTION SYSTEM

E. Sumer [a], M. Turker [b]

[a] Baskent University, Department of Computer Engineering, Eskisehir Road 20.km
06530 Ankara, TURKEY, esumer@baskent.edu.tr
[b] Hacettepe University, Faculty of Engineering, Department of Geodesy and Photogrammetry,
06800 Beytepe, Ankara, TURKEY, mturker@hacettepe.edu.tr

KEY WORDS: Earthquakes, Building, Detection, Aerial, Raster, Vector, Integration, System

ABSTRACT:

An integrated damage detection system, which was developed to detect the collapsed buildings due to Kocaeli earthquake, occurred on 17 August 1999, is introduced. The implementation of the system was carried out in a selected area of the city of Golcuk, TURKEY. The developed system is composed of three components: (i) input, (ii) analysis and (iii) output. In the input component, the post-event panchromatic aerial image of the study area and the vector building boundaries are fed into the analysis component. In the analysis component, an approach, which utilizes the building grey-value and the gradient orientation, is implemented. In the overall assessment of the buildings, the grey-value and the gradient orientation-based results are combined and a single label (collapsed or un-collapsed) is assigned to each building in an integrated manner. In the output component, the results of the total labeling are presented in both graphical and textual mode. The results show that of the 284 buildings analyzed, 254 were labeled correctly as collapsed and un-collapsed providing the producer's accuracies of 81% and 92%, respectively. If the buffer zones are generated around the buildings and the assessments are carried out within the buffered building polygons, 258 buildings are labeled correctly providing the producer's accuracies of 81% and 94%, respectively for the collapsed and un-collapsed buildings. It can be concluded that the collapsed buildings caused by the earthquake can be successfully detected from post-event aerial images using an automated system approach.

1. INTRODUCTION

A strong earthquake (Mw7.4), which is also known as Kocaeli earthquake, struck northwest of Turkey in August 17, 1999. This severe earthquake lasted for about 45 seconds, killing more than 17,000 people and destroying many cities and towns including Yalova, Izmit, Golcuk and Istanbul. In Golcuk, a significant number of multi-story buildings experienced a severe damage including the complete collapse of the buildings (MCEER, 2000). Determining the extent of the damage caused by such a catastrophic event is a vital issue for effective emergency management and allocation of limited resources. Remote sensing becomes an important tool to collect the required information, which provides up-to-date information about the earth surface features. In many applications of damage assessment and building detection, the aerial imagery is widely used due to its broad spectral sensitivity, increased spatial resolution, and geometric fidelity. In addition to that, various kinds of data sources such as nighttime imagery, optical imagery, radar imagery, aerial video imagery, and airborne MSS imagery are frequently used in the post-quake damage assessment studies.

Several studies have been conducted on earthquake damage detection using various data sources. Ishii *et al.* (2002) proposed a two-phase method in order to detect the damaged areas from aerial photographs. In the first phase, the combination of color and edge information was utilized, which provides the discrimination of the damaged areas from the non-damaged. In the second phase, the pre- and post-event aerial imagery of the same area were analyzed by matching them using the affine transformation and also by hand. Then, the colors of the corresponding pixels in each image were checked. Thus, the damaged areas were extracted by calculating the difference of colors of two pixels in the same geographic location. In a similar study carried out by Mitomi *et al.* (2000), the damaged buildings were detected by processing the aerial television images taken after the 1999 Kocaeli, Turkey and Chi-Chi, Taiwan earthquakes. The method was focused on the characteristics of damage based on hue, saturation, brightness and the edge elements. In a different study, a near-real time earthquake damage assessment methodology was proposed by Gamba and Casciati (1998). Their two-phase system provided the integration of GIS and remote sensing. In the first phase, GIS side of the study was performed by collecting and analyzing data about the buildings and infrastructures. In the second phase, the system received near-real time imagery of the suffered area to perform change detection through shape analysis and perceptual grouping using the pre- and post-event aerial images. Turker and San (2003) used pre- and post-event SPOT HRV images to detect the changes due to Izmit earthquake. The change areas were identified by subtracting the near-infrared channel of the merged pre-event image from that of the post-event image. In a recent study, Turker and Cetinkaya (2005) detected the collapsed buildings caused by the 1999 Izmit earthquake using digital elevation models (DEMs) created from the aerial photographs taken before (1994) and after (1999) the earthquake. The DEMs created from two epochs were differenced and the difference DEM was analyzed on a building-by-building basis for detecting the collapsed buildings. Further, Turker and San (2004) utilized the cast shadows to detect the collapsed buildings due to Izmit 1999 earthquake. The existing vector building boundaries were used to match the

shadow casting edges of the buildings with their corresponding shadows and to perform analysis in a building specific manner. In a study conducted by Guler and Turker (2004), the collapsed buildings due to Izmit, Turkey earthquake were detected from post-event aerial photographs using the shadow analysis and perceptual grouping procedure. First, the canny edge detector algorithm was applied to detect the edges between cast shadows and the surroundings. After that, the output edge image was converted into vector line segments. Then, these line segments were grouped together using a two-level hierarchical perceptual grouping procedure. Thus, the damage conditions of the buildings were assessed by measuring the agreement between the detected line segments and the previously known vector building boundaries. Similarly, Sumer and Turker (2004) performed the detection of the collapsed buildings due to Izmit, Turkey earthquake from the post-event aerial imagery using the watershed segmentation algorithm. First, the shadow producing edges of the buildings were identified. Then the shadow and non-shadow regions of the buildings were detected using the watershed segmentation. The extent of the damage was determined by measuring the agreement between the shadow producing edges of the buildings and the corresponding shadows based on the percentage of the shadow pixels.

In this study, we propose a damage detection system in order to identify the collapsed buildings in a selected urban area of the city of Golcuk by integrating the existing vector building boundaries and the post-earthquake aerial imagery. The system was developed using the MATLAB programming language, which enables the handling of the image processing algorithms.

2. STUDY AREA

The implementation of the system was carried out in a selected area of the city of Golcuk, which is one of the urban areas most strongly hit by the Kocaeli earthquake. The region is located on the south coast of Izmit Bay, which is east-west elongated structural basin situated along the North Anatolian Fault (NAF) at the eastern margin of the sea of Marmara. The study area consists of 284 rectangular shaped buildings. Of these buildings, 79 were collapsed while the remaining 205 were un-collapsed (Figure 1).

3. DAMAGE DETECTION SYSTEM

The general architecture of the developed system is illustrated in figure 2. As can be seen in the figure, two different inputs are fed into the analysis component, which are the post-event aerial photograph and the vector building boundaries. In the analysis component, an approach based on building grey-value and gradient orientation is presented. Finally, in the output side, the graphical and textual results are obtained.

Figure 1. Study area

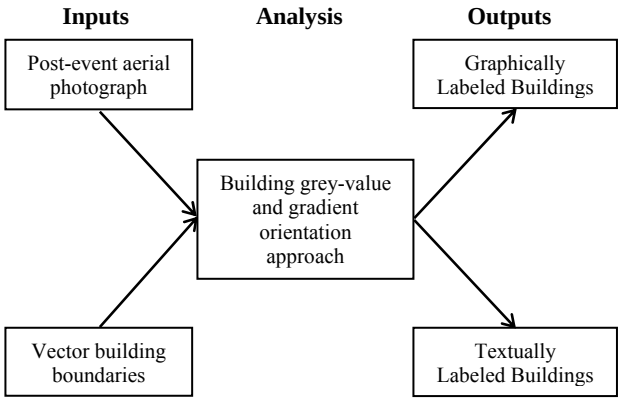

Figure 2. General architecture of the system

3.1 Input Component

The post-event panchromatic aerial image and the vector building boundaries are fed into the analysis component. To implement the approach, the 1-m spatial resolution post-quake aerial photograph supplied by the General Command of Mapping (GCM) of Turkey was used. The post quake aerial photographs (1:16,000) were acquired by GCM in September 1999 and were scanned at 21μm to convert them into digital form (Figure 1). The vector building boundary data set contain, for each building, the Cartesian coordinates of the edge points (Figure 3).

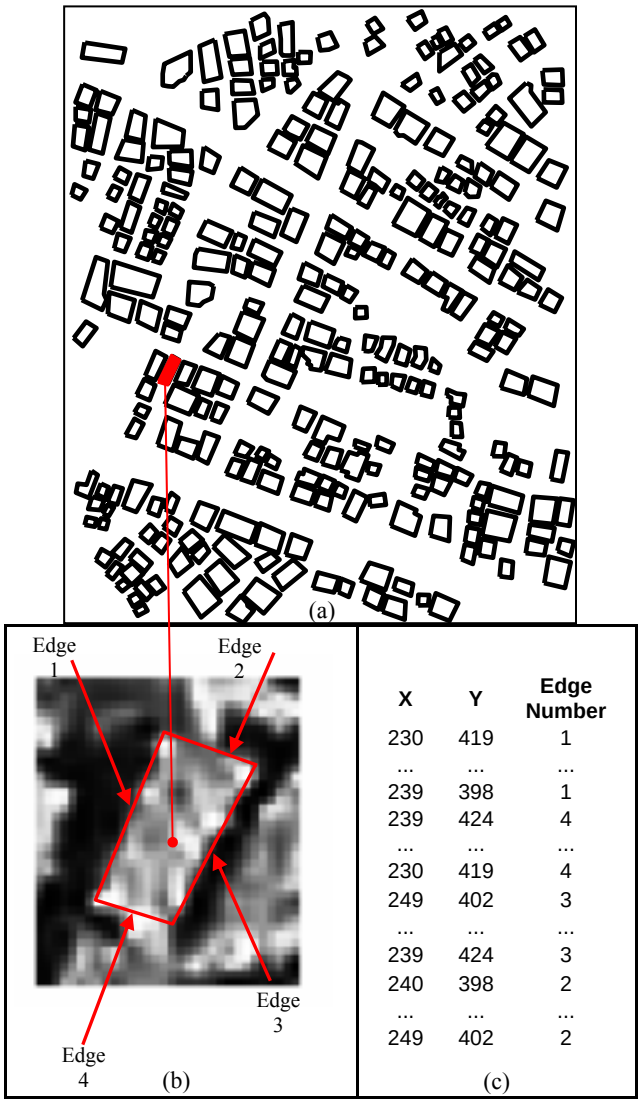

Figure 3. (a) Vector building boundaries, (b) the edges of a building and (c) the structure of vector data

3.2. Analysis Component

The proposed approach for detecting the damaged buildings contains two branches: (i) Building Grey-Value, and (ii) Gradient Orientation.

3.2.1 Building Grey-Value Approach: In this approach, the damage detection process was performed based on the building grey-value information. It was observed that in the study area, the collapsed buildings reflect higher brightness values (BVs) than the un-collapsed ones. The difference in the reflection may be due to the roof type (mostly tile), which appears dark in the panchromatic images. In addition, for un-collapsed buildings, the shadows caused by the slope of the roofs may also diminish the BVs. Therefore, it can be said that the amount of light intensity reflected by the buildings may vary. The BV variation between a collapsed and un-collapsed building is illustrated in figure 4.

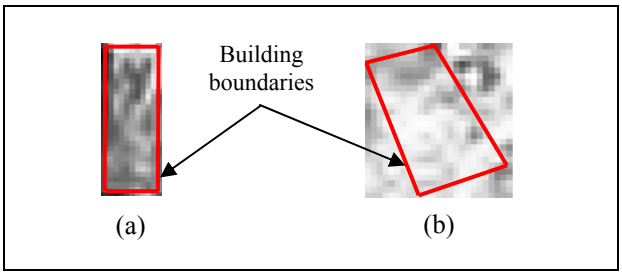

Figure 4. (a) An un-collapsed building with low BV and (b) a collapsed building with higher BV.

In this approach, the first step was to determine a grey-value threshold level (T_{GV}). This was done through analyzing the BVs of the all collapsed and un-collapsed buildings in the reference data. To find the optimum threshold value, the grey-value histograms were generated for both the collapsed and un-collapsed buildings. Then, the intersection of the two normal curves, which give the optimum grey-value threshold, was computed by using the normalization curve (1).

$$y=f(x \mid \mu,\sigma)=\frac{1}{\sigma(2\pi)^{1/2}} e^{\frac{-(x-\mu)^2}{2\sigma^2}}, -\infty < x < \infty \qquad (1)$$

where, μ is the mean value of the normal curve and σ is the standard deviation. In the present case, the optimum threshold level was computed to be 145. This means that the collapsed buildings have an average BV greater than 145. For each building, those pixels that have grey-values above the threshold of 145 (T_{GV} = 145) were counted and divided to total number of pixels contained within the buildings. This value gave us the pixel ratio (PR) per building. For instance, if the number of pixels staying above T_{GV} is 114 and the total number of pixels contained within the building is 256 then, for this building, PR is computed to be 44.53% (114 / 256 = 0.4453).

It was observed that generally the PRs were higher for the collapsed buildings than the uncollapsed. This is because the pixels with high grey-values are frequently encountered within the collapsed buildings. At the end of the analysis, the 60% pixel ratio was accepted to be the optimum threshold level to be used in discriminating the collapsed and un-collapsed buildings. To find the optimum ratio, the error matrices were constructed for the varying pixel ratios, which change between 10% and 90%. By using these matrices, several predefined accuracy indices including the overall accuracy, overall kappa, average user's and producer's accuracies, and combined user's and producer's accuracies were computed. Most of these indices provided the highest percentage for the PR level of 60%. Therefore, 60% was chosen to be the optimal PR.

3.2.2 Gradient Orientation Approach: This approach is based on the detection of the variation in the gradient direction for each building image patch. It is assumed that, for collapsed buildings, the direction of gradient is randomly distributed. On the other hand, for un-collapsed buildings, the orientation of the gradient is assumed to be more regular and concentrated in a few directions (Figure 5). This assures that the collapsed buildings can be discriminated from the un-collapsed by

analyzing the angle information of the gradient image of the buildings.

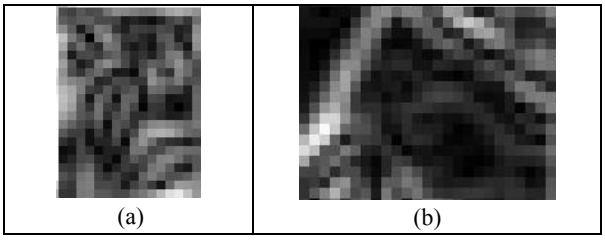

(a) (b)

Figure 5. (a) A collapsed building with random gradient directions and (b) an un-collapsed building with regular gradient patterns

In the first step, the vertical and horizontal partial derivatives were computed by averaging the finite differences over a 2x2 square array (2).

$$P(x,y) \approx (I(x,y+1) - I(x,y) + I(x+1,y+1) - I(x+1,y)) / 2$$
$$Q(x,y) \approx (I(x,y) - I(x+1,y) + I(x,y+1) - I(x+1,y+1)) / 2 \quad (2)$$

where, P(x,y) and Q(x,y) are the vertical and horizontal partial derivatives, respectively and I(x,y) is the original image. Then, the magnitude and the orientation of the gradient were calculated (3).

$$M(x,y) \approx (P(x,y)^2 + Q(x,y)^2)^{1/2}$$
$$\theta(x,y) \approx \arctan(Q(x,y), P(x,y)) \quad (3)$$

where, M(x,y) is the magnitude of the gradient and θ(x,y) is the orientation of the gradient. The function arctan (x,y) computes an angle between [-π, +π]. However, in the present study, this range is mapped into [0, +π]. The partial representation of the gradient magnitude and the orientation (for each pixel) are illustrated in figure 6, where the numbers represent, for the corresponding pixels, the angles between 0^o and 180^o.

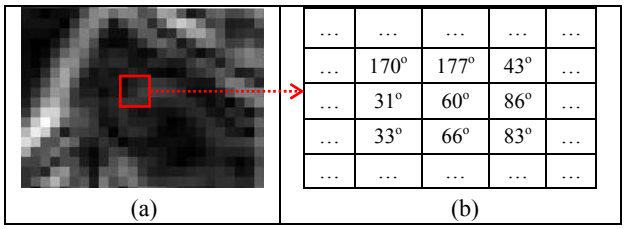

(a) (b)

Figure 6. (a) The gradient magnitude and (b) the gradient orientation (in degrees) of a selected area of a building patch

After obtaining the gradient orientation, the whole angle range (0^o - 180^o) was divided into 15^o subintervals, which were 0-15, 16-30, 31-45, 46-60, 61-75, 76-90, 91-105, 106-120, 121-135, 136-150, 151-165 and 166-180. Then, for each building, the gradient direction histograms were generated. In these histograms, the abscissa represents the gradient direction from 0^o to 180^o divided into 12 equal intervals, while the ordinate represents the frequency of the gradient directions (Figure 7).

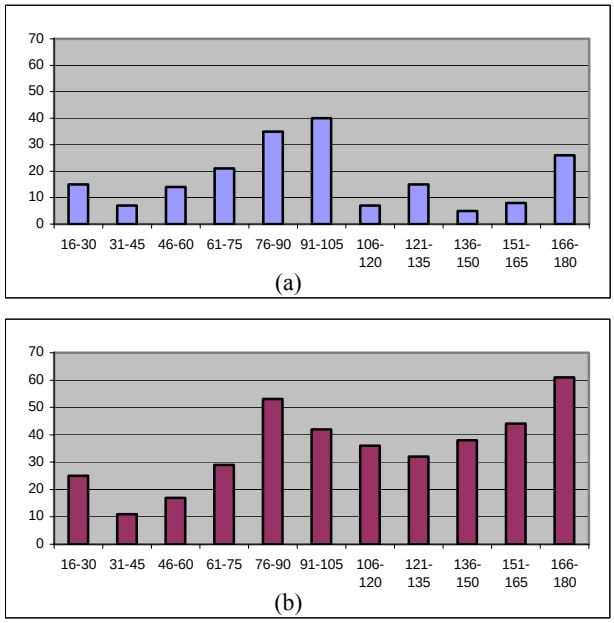

Figure 7. (a) An un-collapsed building and (b) a collapsed building with unbiased frequencies

It can be observed in figure 7 that the interval (0^o-15^o) was not taken into account due to its high frequency, which causes a biased distribution. After the elimination of this interval, the histogram of a collapsed building looks relatively flat compared with the histogram of an un-collapsed building.

The last step was finding an optimum standard deviation threshold level (T_{SD}) that discriminates the collapsed buildings from the un-collapsed. To do that, the average of the standard deviation values of all collapsed and un-collapsed buildings were computed to be 16.07 and 17.93, respectively. Then, T_{SD} was found to be 17 by computing the intersection of the two normal curves as described previously.

3.2.3 Assessments of the Building Conditions by Combining the Two Approaches

The final decision about the building condition was made by combining the threshold levels found in the building grey-value and the gradient orientation approaches. A building was marked collapsed if the PR computed for it was above the threshold of 60% and the standard deviation of the gradient direction distribution was below the optimum T_{SD} of 17. Otherwise, the building was labeled un-collapsed.

3.3 The Results and the Output Component

All the buildings falling within the study area were assessed. Of the 284 buildings, 254 were correctly detected by the proposed integrated damage detection system. The error matrix, which includes the overall accuracy, the user's and producer's accuracies for collapsed and un-collapsed buildings, is illustrated in table 1.

	Reference		
	Collapsed	Un-collapsed	Total
Collapsed	64	15	79
Un-collapsed	15	190	205
Total	79	205	284
Producer's Accuracy (%)	**81,01**	**92,68**	
User's Accuracy (%)	**81,01**	**92,68**	
Overall Accuracy (%)	**89,44**		

Table 1. The error matrix computed using the optimum PR and the standard deviation threshold level (T_{SD}).

The overall accuracy was computed as 89.44%. For un-collapsed buildings, both the producer's and user's accuracies were found to be 92.68%. For collapsed buildings, the user's and producer's accuracies were same (81.01%). It can be observed that due to several reasons 30 buildings were not detected correctly. The erroneously detected buildings represent omission and commission errors.

The output component of the developed damage detection system yields two forms of output. The first output is in textual form (Table 2).

Optimum Standard Deviation Threshold Level (T_{SD}): **17**
Optimum Pixel Ratio (PR): **60%**

Pixel Ratio: 47.27%
Standard Deviation: 13.15

Analysis: Building # 2 is UN-COLLAPSED
Ground Truth: Building # 2 is UN-COLLAPSED

Pixel Ratio: 82.43%
Standard Deviation: 7.50

Analysis: Building # 3 is COLLAPSED
Ground Truth: Building # 3 is COLLAPSED

Table 2. A sample textual output for the buildings #2 and #3.

In table 2, the buildings #2 and #3 were labeled un-collapsed and collapsed through the proposed building grey-value and gradient orientation analyses approaches. These labels were compared with the ground truth information and an agreement was observed between them. Therefore, for these buildings, the labels were said to be correct.

The second type of output is in the graphic form, which illustrates the damage conditions of the buildings graphically. To do this, four distinct colors were used for representing the conditions of the buildings. While the green and red colors represent the un-collapsed and collapsed buildings, the blue and yellow colors represent the erroneously detected buildings, which are the omission and commission errors in the error matrix. The omission error means that the collapsed buildings were detected as un-collapsed. On the other hand, the commission error means that the un-collapsed buildings were labeled as collapsed. These error types are illustrated in figure 8.

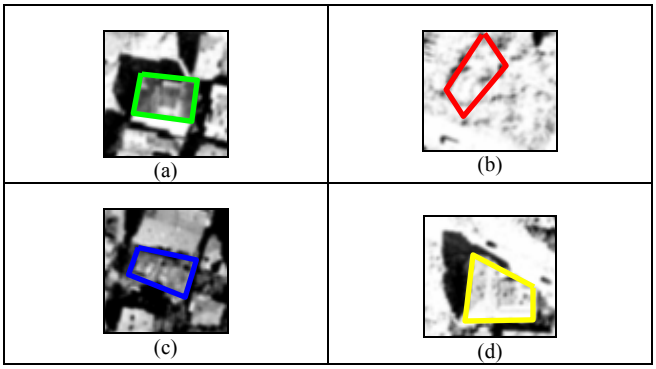

Figure 8. (a) Un-collapsed building, (b) collapsed building, (c) omission error, and (d) commission error.

In the last part of the study, an improvement was made on the proposed approaches. This was achieved by generating a one-pixel wide buffer region around the boundaries of the vector building polygon (Figure 9). The purpose for generating the buffer zone was to improve the accuracy of the proposed damage detection system.

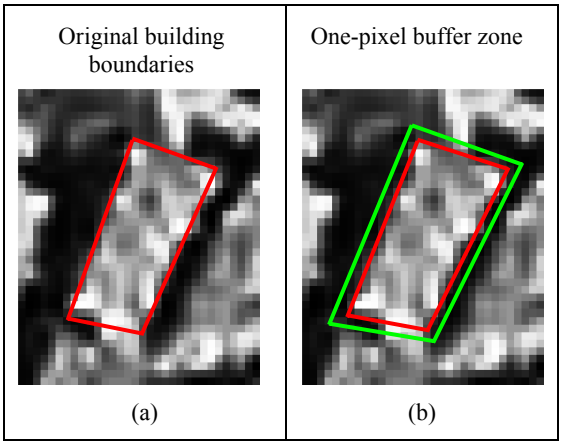

Figure 9. A building polygon (a) with no buffer zone and (b) with one-pixel buffer zone.

The reasons for selecting the size of the buffer zone as one pixel are twofold: (i) generating a buffer zone wider than one pixel may increase the chance of the inclusion of the unnecessary shadow areas cast by the building under consideration and (ii) the buffer zone wider than one pixel may increase the chance of the inclusion of the undesired building areas and the shadow areas of the neighboring buildings.

As in the without buffer case, the threshold levels required to perform the analyses were also computed in the buffer case (when a one pixel wide buffer zone is generated). For the buffer case, the optimum grey-value threshold level (T_{GV}) was computed to be 141. On the other hand, the optimum pixel ratio (PR) and the optimum standard deviation threshold level (T_{SD}) were found to be 60% and 17.31, respectively. Therefore, the analyses of the buildings were repeated using the PR value of 60% and the optimum standard deviation threshold level of 17.31. The results given in table 3 as an error matrix reveal that

of the total 284 buildings analyzed, 258 were correctly labeled yielding an overall accuracy of 90.85%. Furthermore, for collapsed buildings, the producer's and user's accuracies were computed to be 81.01% and 85.33%, respectively. For un-collapsed buildings, the producer's and user's accuracies were found to be 94.63% and 92.82%, respectively. As can be seen in the error matrix, 26 buildings were not detected correctly. Of these erroneously detected 26 buildings, 15 were not detected as collapsed. Instead, 11 un-collapsed buildings were detected as collapsed. In each case, the erroneously detected buildings represent the omission and commission errors, respectively

	Reference		
	Collapsed	Un-collapsed	Total
Collapsed	64	11	75
Un-collapsed	15	194	209
Total	79	205	284
Producer's Accuracy (%)	**81,01**	**94,63**	
User's Accuracy (%)	**85,33**	**92,82**	
Overall Accuracy (%)	**90,85**		

Table 3. The error matrix computed from the analyses of the buffered buildings

4. CONCLUSIONS

In this study, an integrated damage detection system was introduced. The analysis component of the system contains a two branch decision mechanism for labeling the damage conditions of the buildings. While in the first branch the decision is made based on building grey values, in the second branch the gradient orientation procedure is used. The developed system was implemented in the city of Golcuk, which is one of the urban areas most strongly affected by the 1999 Izmit earthquake. The results achieved are satisfactory. The overall accuracy was computed to be 89.44%. On the other hand, for the collapsed and un-collapsed buildings, the producer's accuracies were found to be 81.01% and 92.68%, respectively. In the output component, the visualization of the labeled buildings was provided by textual and graphical outputs.

In order to improve the accuracy, one pixel wide buffer zone was generated around the building polygons and the damage assessments were re-performed. It was found that the overall accuracy increased to 90.85%. On the other hand, for the collapsed and un-collapsed buildings, the producer's accuracies were computed to be 81.01% and 94.63%, respectively. It was observed that for un-collapsed buildings, the producer's accuracy was improved when one-pixel wide buffer region is included in the assessments.

The major benefit of the developed system is that it provides an automatic detection of the collapsed buildings efficiently and effectively on building-by-building basis. The integration of the post-quake raster aerial image and the vector building boundary data appears to be very useful as it increases the overall and producer's accuracies. It can be stated that the collapsed buildings caused by the earthquake can be successfully detected from post-event aerial images using an automated system approach.

5. REFERENCES

Gamba, P. and Casciati, F., 1998. GIS and Image Understanding for Near-Real-Time Earthquake Damage Assessment. *Photogrammetric Engineering and Remote Sensing*, 64(10), pp. 987-994.

Guler, M. A. and Turker, M., 2004. Detection of the Earthquake Damaged Buildings from Post-event Aerial Photographs using Perceptual Grouping. *Proceedings of XXth International Society for Photogrammetry and Remote Sensing (ISPRS'04) Congress*, Commission III, July 12-23, Istanbul, TURKEY.

Ishii, M., Goto, T., Sugiyama, T., Saji, H. and Abe, K., 2002. Detection of Earthquake Damaged Areas from Aerial Photograph by Using Color and Edge Information. *Proceedings of the Fifth Asian Conference on Computer Vision*, pp. 27-32.

MCEER (Multidisciplinary Center for Earthquake Engineering Research), 2000. The Marmara, Turkey Earthquake of August 17,1999: Reconnaissance Report, Technical Report MCEER-00-0001, University of Buffalo, State University of New York.

Mitomi, H., Yamazaki, F. and Matsuoka, M., 2000. Automated Detection of Building Damage due to Recent Earthquakes Using Aerial Television Images. *21st Asian Conference on Remote Sensing*, Vol. 1, pp. 401-406.

Sumer, E. and Turker, M., 2004. Building Damage Detection from Post-Earthquake Aerial Images Using Watershed Segmentation in Golcuk, Turkey. *Proceedings of XXth International Society for Photogrammetry and Remote Sensing (ISPRS'04) Congress*, Commission VII, July 12-23, Istanbul, TURKEY.

Turker, M. and Cetinkaya, B., 2005. Automatic detection of earthquake damaged buildings using DEMs created from pre- and post-earthquake stereo aerial photographs. *International Journal of Remote Sensing*, 26(4), pp. 823-832.

Turker, M. and San, B.T., 2004. Detection of collapsed buildings caused by the 1999 Izmit, Turkey earthquake through digital analysis of post-event aerial photographs. *International Journal of Remote Sensing*, 25(21), pp. 4701-4714.

Turker, M. and San, B.T., 2003. SPOT HRV data analysis for detecting earthquake-induced changes in Izmit, Turkey. *International Journal of Remote Sensing*, 24(12), pp. 2439-2450.